Some Unrelated Topics of Interest

Michael Trott

April 5, 2001

1 High-precision Value for the Quartic Anharmonic Oscillator Ground State

1.1 Introduction

As is well known, only a very limited number of one–dimensional potentials allow for an exact solution of the Schrödinger equation[1]. This means that for many model potentials one has to resort to numerical solution methods. For judging their accuracy, reliability, and speed it is important to have high–precision values of certain nonexactly solvable potentials. The most investigated of such potentials is the quartic anharmonic oscillator [1-11][12-19] described by

$$-\psi_k''(z) + z^4\,\psi_k(z) = \varepsilon_k\,\psi_k(z) \tag{1}$$

The eigenfunctions to the eigenvalues ε_k decay exponentially for $z \to \pm\infty$.

1.2 The Hill Determinant Method

A classical method to solve Sturm–Liouville problems of type 1 is to calculate the eigenvalues of a truncated version of the corresponding Hill determinant. Using the harmonic oscillator basis $\phi_n(z)$ we write $\psi_0(z) = \sum_{k=0}^{\infty} \alpha_k\,\phi_k(z)$ where

$$-\phi_k''(z) + z^2\,\phi_k(z) = \epsilon_k\,\phi_k(z) \tag{2}$$

$$\phi_n(z) = \frac{1}{\sqrt{\sqrt{\pi}\,2^n\,n!}}\,e^{-\frac{z^2}{2}}\,H_n(z) \tag{3}$$

Forming the matrix elements $h_{m,n} = \int_{-\infty}^{\infty} \phi_m(z) \left(-\phi_n''(z) + z^4 \phi_n(z)\right) dz$. For $n \geq m$ we obtain

$$h_{m,n} =$$

$$
\begin{cases}
0 & n - m > \\
2^{\frac{m-n}{2}-4} \sqrt{\frac{m!}{n!}} \left(32\, n\, \delta_{m,n-2}\, (n-1)^2 + 16\,(n-3)\,(n-2)\,n\,\delta_{m,n-4}\,(n-1) + \right. & \text{else} \\
\left. 4\,(2\,n\,(3\,n+5)+5)\,\delta_{m,n} + 8\,(n+1)\,\delta_{m,n+2} + \delta_{m,n+4}\right)
\end{cases}
\tag{4}
$$

A rough estimation shows that one obtains about 0.2 digits per harmonic oscillator state. So by taking into account the first 500 eigenstates and carrying out the calculation with about five thousand digits one obtains about 120 reliable digits for ε_0. (This calculation takes about 20 minutes on a 2000 vintage workstation using *Mathematica* 4 [20].)

$$\varepsilon_0 =$$
$$1.06036209048418289964704601669266354551520872852897793321624\overset{\cdot\cdot}{5}.$$
$$24169594356304434442112689629913467170351054624435858252558\overset{\cdot\cdot}{0}.$$
$$982763829\ldots$$

The Hill determinant approach allows in addition to the calculation of the eigenvalues, the calculation of the eigenvectors. The following graphic visualizes the matrix of eigenvectors of $(h_{m,n})_{1\leq n,m\leq 100}$. The graphic shows that the lowest eigenfunctions are quite similar to the harmonic oscillator eigenfunctions. Higher states are complicated mixtures of harmonic oscillator states. The overall "checkerboard"–like structure results from the fact that the contribution of the antisymmetric (symmetric) harmonic oscillator states to the symmetric (antisymmetric) anharmonic oscillator states is identical zero. The very high states are dominated by truncation effects and do not correctly mimic the anharmonic oscillator states.
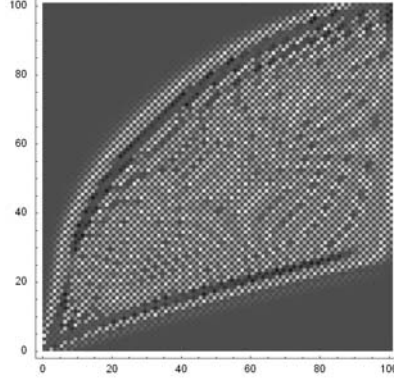
Figure 1: The matrix of eigenvectors of $(h_{m,n})_{1 \leq n,m \leq 100}$.

1.3 The New Algorithm

To get a very high–precision approximation of

$$-\psi''(x) + z^4\,\psi(x) = \lambda\,\psi(x) \tag{5}$$

we start with the series expansion

$$\psi(x) = y_n(x) = \sum_{k=0}^{n} a_k(\lambda)\,x^k \tag{6}$$

For the ground state we choose (ignoring normalization) $\psi(0) = 1$, $\psi'(0) = 0$. For "suitable chosen" x^* we then find high–precision approximations for the zeros of $y_n(x^*)$ and $y'_n(x^*)$. These zeros then bound λ_0 from below and above.

Using the differential equation one obtains the following recursion relation for the $a_k(\lambda)$:

$$a_k(\lambda) \;=\; \frac{a_{m-6}(\lambda) - \lambda\,a_{m-2}(\lambda)}{m^2 - m} \tag{7}$$

For large n $(n \to \infty)$ we want the function $y_n(x)$ to vanish as $x \to \infty$. For a λ smaller than the smallest possible λ, the function $y_n(x^*)$ will not have a zero, but the function $y'_n(x^*)$ will have a zero for a certain x^*. For a λ larger than the smallest possible λ, the function $y_n(x^*)$ will have a zero, but the function $y'_n(x^*)$ will not have a zero for a certain x^*. This allows to find a bounding interval for λ_0. The next two graphics show $y_{80}(x)$ and $y'_{80}(x)$ for 10 equidistant values for λ from the interval [1.05, 1.08] to visualize this bounding process. (For more details, see [21].)
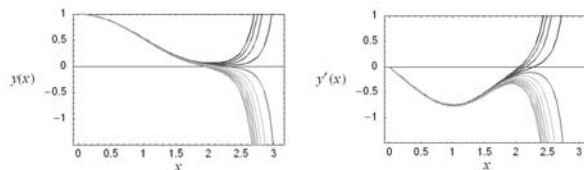
3

Figure 2: $y_{80}(x)$ and $y'_{80}(x)$ for 10 equidistant values for λ from the interval [1.05, 1.08].

It is straightforward to implement the calculation of the bounding interval for λ_0 in *Mathematica* in a three–line program (see [22]). Using `FindRoot` we calculate high–precision values for the zeros of $y_n(\xi)$ and $y'_n(\xi)$.

```
λBounds[n_, ξ_, opts___] :=
   Function[f, λ /. FindRoot[f[n, λ, ξ] == 0,
      {λ, 106/100, 107/100}, opts]] /@ {y, yPrime};
```

The calculation of $y_n(\xi)$ and $y'_n(\xi)$ is also straightforward based on a recursive calculations of the $a_k(\lambda)$.

```
y[n_, λ_Real, ξ_] := Module[{a6, a4, a2, ak, σ},
   {a6, a4, a2} = {1, -λ/2, λ^2/24};
    σ = a6 + a4*ξ^2 + a2*ξ^4;
    Do[ak = a6 - λ*(a2/(k*(k - 1)));
      {a6, a4, a2} = {a4, a2, ak};
      σ = σ + ak*ξ^k, {k, 6, n, 2}]; σ]

y[n_, λ_Real, ξ_] := Module[{a6, a4, a2, ak, σ},
   {a6, a4, a2} = {1, -λ/2, λ^2/24};
    σ = a6 + 2*ξ*a4 + 4*ξ^3*a2;
    Do[ak = a6 - λ*(a2/(k*(k - 1)));
      {a6, a4, a2} = {a4, a2, ak};
      σ = σ + k*ak*ξ^(k - 1), {k, 6, n, 2}]; σ]
```

Calculating now λ`Bounds[16000, 16, `*startingValues*`, WorkingPreci`∤ `sion→6000, AccuracyGoal→600, MaxIterations→100]` (where *startingValues* has been obtained from a call to λ`Bounds` recursively, one gets in a few minutes a 1184 digit approximation to the ground state energy of the quartic anharmonic oscillator.

$$\varepsilon_0 =$$
1.0603620904841828996470460166926634551520872852897793321624\5⋰.
241695943563044344421126896299134671703510546244358582525580⋰.
879808210293147013176836373824935789226246004708175446960141⋰.
637488417282256905935757790888061788790263601549395690275196⋰.
148900942934873584409442694897901213971464290951923354533828⋰.

3470335057576151120257039888523720240221841103086573731091390
891545365841031116794058335486000922744006963112670238862297
142969961059215583226671376935508673610000831830027517926233
573913906136180776498596961814994127928092728407079561060440
722946809949136275729273872791368902798424722261716944488954
751370438068405439187787729532342458743725431783231906038106
874160440343745301468472781391861294047043103401351071607110
353008929823275427661518986950565047160252756089526262191025
688200964410287815640052705292932405076382650282591124773625
384718547144025722854384852974504585709788402490669995704768
445877091762029124375273254907116433440230294730692398190895
685374535988446016002313291933059395869304916644281633946163
324287004261461237743009952234204208597735690153565416850308
941851348795734106585479719467596466796613467688586437952654
    519560568286715958338884743467012042420714919290048732…

Statistical analysis of the number does not show any regularity.

1.4   Summary

A power series based approach to the high–precision calculation of the ground state of the anharmonic oscillator was presented. *Mathematica* code to carry out the calculation, as well as results were given. The method can straightforwardly be used to calculate ten thousands of digits of the quartic anharmonic, as well as other anharmonic oscillators. Work concerning the application of the method to higher states is in progress.

All calculations and visualizations have been carried out in *Mathematica* 4.

1.5   Local Density of States for the Harmonic Oscillator

The next graphic shows the local density of states $\mathcal{D}_E(x) = \langle x \,|\, \theta(E - \hat{H}) \,|\, x \rangle$ for the harmonic oscillator [21].
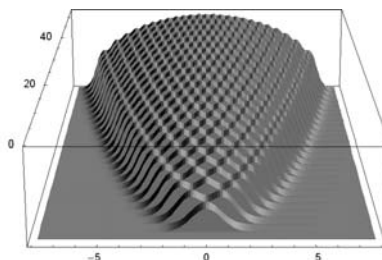
Michael Trott

Figure 3: The local density of states $\mathcal{D}_E(x) = \langle x \,|\, \theta(E - \hat{H}) \,|\, x \rangle$ for the harmonic oscillator.

1.6   Acknowledgments

2   Are Brillouin Zones of High Order Fractal?

2.1   Introduction

Brillouin zones are among the most popular objects a solid state physicist deals with [23-26]. Despite the fundamental importance for the explanation of most properties of crystalline solids, Brillouin zones as an own subject have rarely been investigated (the only ones we are aware of are [27-30]). For electronic properties, mostly the low order Brillouin zones matter, as an ownstanding subject the high order Brillouin zones are interesting. Mathematically, the $(n + 1)$th Brillouin zone is the set of points that a line to them crosses exactly n bisector planes. In computational geometry a nth order Brillouin zones is also called nth degree Voronoi region or nth nearest point Voronoi diagrams. The most important fact for high order Brillouin zones is that their shape approaches that of a thin spherical shell and their volume is a constant. Here, for the first time we report on some computational results of higher order Brillouin zones. All calculations and visualizations were done with *Mathematica* 4 [20].

Recursive definition of Brillouin zones: Given a lattice Λ in $\mathbb{R}^d$ with lattice points $\boldsymbol{h}_i$ (i being a multiindex) the first Brillouin zone $\mathcal{BZ}_1$ is the closure of the set of all

points x such that $|x - 0| \leq |x - h_i|$ for all $h_i \neq 0$. The nth order Brillouin zones is the closure of the set of all points x such that $|x - 0| \leq |x - h_i|$ for all $h_i \neq 0$ and $x \notin \mathcal{BZ}_{n-1}$.

2.2 2D Hexagonal Lattice

Figure 4 shows the first twenty Brillouin zones of a 2D hexagonal lattice. It is interesting to observe that the first, third, and fourth Brillouin zones have the shape of an hexagon. For higher orders the shape becomes much more complicated.
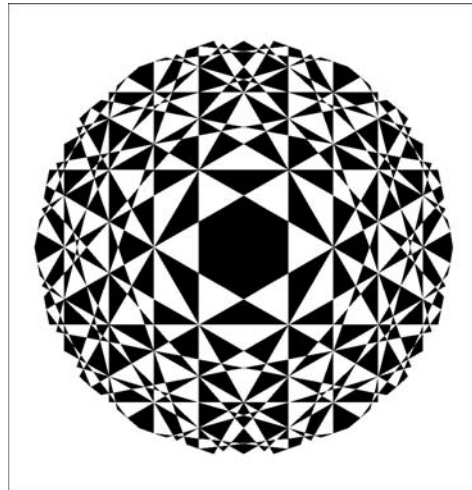

Figure 4: The first twenty Brillouin zones of a 2D hexagonal lattice.

Figure 5 shows the 200th Brillouin zone in one symmetry unit (inside an angle of 30°). One sees many small and a few quite large Landsberg zones. The distribution $p(A)$ of the area of the Landsberg zones in the limit $n \to \infty$ might be an interesting subject to study.
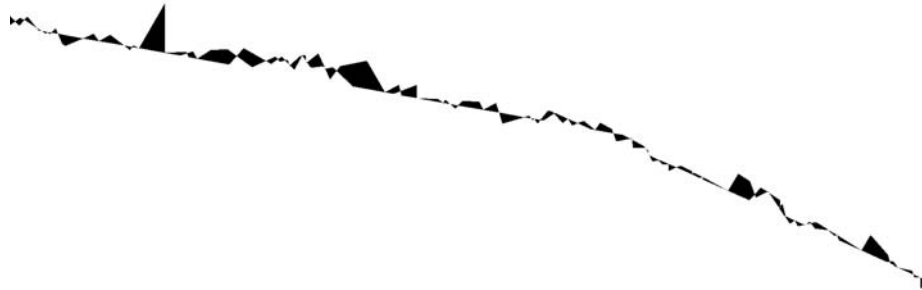
Figure 5: The 200th Brillouin zone in one symmetry unit (inside an angle of 30°).

A good numerical fit to number of faces (line segments) $\sharp_n$ of the nth Brillouin zone is $\sharp_n \propto n^{1.15}$. Figure 6 shows the circumference of the Brillouin zones normalized to the circumference of a circle with the same radius. Does the ratio approach a finite value in the limit $n \to \infty$?
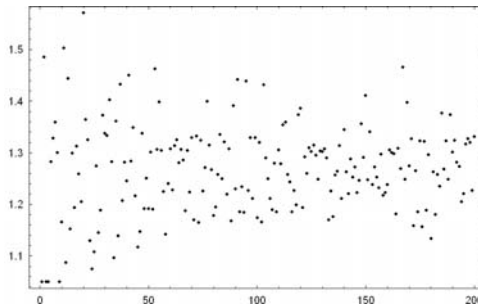

Figure 6: The circumference of the Brillouin zones normalized to the circumference of a circle with the same radius.

2.3   3D Cubic Lattices

In [31] we gave a complete implementation for the effective calculation of higher order Brillouin zones of the three cubic lattice in $\mathbb{R}^3$. Figure 7 shows the (outside of) 15th Brillouin zone for the simple cubic, Figure 8 shows the 18th for the face–centered cubic and Figure 9 shows the 10th for the body–centered cubic lattice. The higher order Brillouin zones show quite complicated behavior. Large faces alternate with small ones, relatively plane regions alternate with quite structured ones. The appearance of the $n+1$th Brillouin zone is typically completely independent of the appearance of the nth Brillouin zone.
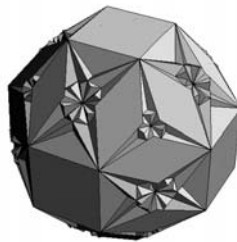
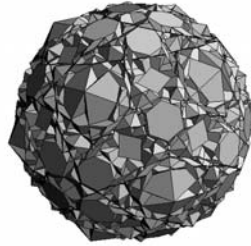Figure 7: The (outside of) 15th Brillouin zone for the simple cubic.

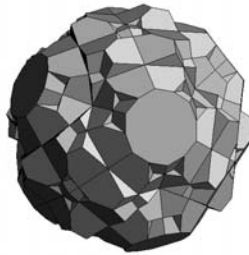Figure 8: The (outside of) 18th Brillouin zone for the face–centered cubic.

Figure 9: The (outside of) 10th Brillouin zone for the body–centered cubic lattice.

Using this implementation we analysed various properties of higher order Brillouin zones. Figure 10 shows the area of the Brillouin zones normalized to the area of a sphere of the same volume. The order of the three curves from the bottom is sc, fcc, bcc.
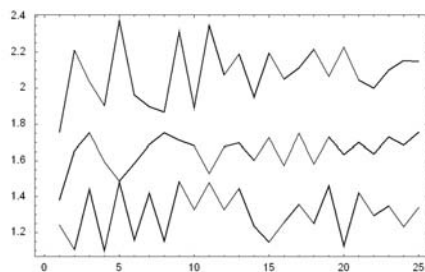
Some Unrelated Topics of Interest

Figure 10: The area of the Brillouin zones normalized to the area of a sphere of the same

The last result to be given here is the number of faces of the Brillouin zones. By a face we mean any connected planar part of the outside facing side of a Brillouin zone (point contacts separate faces). Table 1 gives the results for the first 25 Brillouin zones.

Table 1. The results for the first 25 Brillouin zones.

n	sc	fcc	bcc
1	6	14	12
2	12	72	48
3	72	96	30

Table 2. The results for the first 25 Brillouin zones.

n	sc
1	6

Table 3. The results for the first 25 Brillouin zones.

n	sc	fcc
1	6	14
2	12	72

Table 4. The results for the first 25 Brillouin zones.

n	sc	fcc	bcc	bcc
1	6	14	12	12
2	12	72	48	48
3	72	96	30	30

2.4 Summary

Preliminary results about some computational results about higher order Brillouin zones have been presented. Further work is in progress and will be published elsewhere.

All calculations and visualizations have been carried out in *Mathematica* 4.

2.5 Acknowledgments

The author would like to take the opportunity to thank Amy Young for assistance in typesetting this paper.

A Index Gymnastics

The technique of extracting the content from geometric (tensor) equations by working in component notation and rearranging indices as required[2]. Index gymnastics is a fundamental component of special and general relativity [32]. Examples of index gymnastics include

$$S^{\alpha\beta}{}_{\gamma} = g^{\beta\mu}\, S^{\alpha}{}_{\mu\gamma} \tag{A1}$$

$$S^{\alpha}{}_{\mu\gamma} = g_{\mu\beta}\, S^{\alpha\beta}{}_{\gamma} \tag{A2}$$

$$A^2 = A^{\alpha}\, A_{\alpha} \tag{A3}$$

Some Unrelated Topics of Interest

$$g_{\alpha\beta}\, g^{\beta\gamma} = \delta_\alpha{}^\gamma \qquad\qquad (A4)$$

$$N^\alpha{}_\beta{}^{,\gamma} = N^\alpha{}_{\beta,\mu}\, g^{\mu\gamma} \qquad\qquad (A5)$$

$$(R_\alpha\, M_\beta)_{,\gamma} = R_{\alpha,\gamma}\, M_\beta + R_\alpha\, M_{\beta,\gamma} \qquad\qquad (A6)$$

$$F_{[\alpha\beta]} = \frac{1}{2}\, (F_{\alpha\beta} - F_{\beta\alpha}) \qquad\qquad (A7)$$

$$F_{(\alpha\beta)} = \frac{1}{2}\, (F_{\alpha\beta} + F_{\beta\alpha}) \qquad\qquad (A8)$$

[32], where g_{ij} is the metric tensor, $\delta_\alpha{}^\gamma$ is the Kronecker delta, , is a comma derivative, $F_{[\alpha\beta]}$ is the antisymmetric tensor part, and $F_{(\alpha\beta)}$ is the symmetric tensor part[3].

Notes

[1] This footnote was not added by the author, but was placed for the purpose of demonstration.

[2] From MathWorld, http://mathworld.wolfram.com

[3] See also: Index, Index Lowering, Index Raising, Tensor.

References

[1] Tymczak, C. J., Japaridze, G. S., Handy, C. R., & Wang, X. Q. (1998, March 14). *New perspective on inner product quantization*. Phys. Rev. Lett., **80**(17), 3673–3677.

[2] Graffi, S., & Grecchi, V. (1973, November 15). *Rayleigh-Ritz Method, Secular Determinant, and Anharmonic Oscillators*. Phys. Rev. D, **8**(10), 3487–3492.

[3] Sergeev, A. V., & Goodson, D. Z. (1998, March 14). *Bloch electrons in a magnetic field*. J. Phys., **A**(31), 4301–4301.

Michael Trott

[4] Suzuki, J. (1999, March 14). *A new ambient pressure organic superconductor based on BEDT-TTF with 10.4-K higher than 10K*. J. Phys., **A**(32), 183–187.

[5] Chebotarev, L. V. (1997, Dec 12). *Parabolic connection formulae in quantum mechanics*. Ann. Phys., **255**(2), 305–332.

[6] Shanley, P. E. (1988, March 14). *Large-order analysis of the convergent renormalized strong-coupling perturbation theory for the quartic anharmonic oscillator*. Ann. Phys., **186**(3), 292–325.

[7] Hatsuda, T., Kunihiro, T., & Tanaka, T. (1997, April 28). *Optimized Perturbation Theory for Wave Functions of Quantum Systems*. Phys. Rev. Lett., **78**(17), 3229–3230.

[8] Weniger, E. J. (1996, September 30). *Construction of the Strong Coupling Expansion for the Ground State Energy of the Quartic, Sextic, and Octic Anharmonic Oscillator via a Renormalized Strong Coupling Expansion*. Phys. Rev. Lett., **77**(14), 2859–2862.

[9] Ho, K. C., et al. (1996, March 12). *Study of quantum anharmonic oscillators by state-dependent diagonalization*. Phys. Rev. A., **53**(3), 1280–1284.

[10] Čizek, J., Weniger, E. J., Bracken, P., & Špiro, V. (1996, Dec 12). *Effective characteristic polynomials and two-point Padé approximants as summation techniques for the strongly divergent perturbation expansions of the ground state energies of anharmonic oscillators*. Phys.Rev., **53**(3), 2925–2939.

[11] Bay, K., & Lay, W. (1997, Dec 12). *The spectrum of the quartic oscillator*. J. Math. Phys., **38**(5), 2127–2131.

[12] Voros, A. (1999, March 14). *Magnetic field dependence of the cyclotron effective mass in the organic superconductor*. J. Phys., **32**(A), 5993–6000.

[13] Khan, P. B., & Zarmi, Y. (1999, Dec 12). *Properties of new organic conductors*. J. Math. Phys., **40**(1), 4658–4659.

[14] Antonsen, F. (1997, Dec 12). *Quantum theory in curved spacetime using the Wigner function*. Phys. Rev. D., **56**(2), 920–935.

[15] Skála, L., Čizek, J., Kapsa, V., & Weniger, E. J. (1997, December). *Large-order analysis of the convergent renormalized strong-coupling perturbation theory for the quartic anharmonic oscillator*. Phys. Rev. A, **56**(6), 4471–4476.

[16] Meißner, H., & Steinborn, E. O. (1997, March 14). *Large-order analysis of the convergent renormalized strong-coupling perturbation theory for the quartic anharmonic oscillator*. Phys. Rev., **56**(A), 4471–4476.

[17] Delabaere, E., & Pham, F. (1997, Dec 12). *Unfolding the quartic oscillator*. Ann. Phys, **261**(2), 180–218.

Some Unrelated Topics of Interest

[18] Fernández, F., & Guardiola, R. (1993, Dec 12). *Accurate eigenvalues and eigenfunctions for quantum-mechanical anharmonic oscillators*. J. Phys. A., **26**(23), 7169–7180.

[19] Vinette, F., & Čizek, J. (1991, March 14). *Spinless fermions on frustrated lattices in a magnetic field*. J. Math. Phys., **26**(3), 3392–3396.

[20] Wolfram, S. (1999). *The Mathematica Book*. Champaign: Cambridge University Press and Wolfram Media.

[21] Trott, M. (2000). *The Mathematica GuideBook: Mathematics in Mathematica*. New York: Springer-Verlag.

[22] Trott, M. (2000). *The Mathematica GuideBook: Programming in Mathematica*. New York: Springer-Verlag.

[23] Brillouin, L. (1946). *Wave Propogation in Periodic Structures*. New York: McGraw-Hill.

[24] Ashcroft, N. W., & Mermin, N. D. (1976). *Solid State Physics*. Philadelphia: Saunders College.

[25] Crackwell, A. P., & Wong, K. C. (1973). *The Fermi Surface*. Oxford: Clarendon Press.

[26] Landsberg, P. T. (1969). *Solid State Theory*. London: Wiley.

[27] Bieberbach, L. (1939, Dec 12). *Über die Inhaltsgleichheit der Brillouinschen Zonen*. Monatsh. Math. Phys., **48**(1), 509–515.

[28] Jones, G. A. (1984, Dec 12). *An algorithm for machine calculation of complex Fourier series*. Bull. London Math. Soc., **16**(1), 241–242.

[29] Skriganov, M. M. (1984, March 14). *Mulliken-Wolfsberg-Helmholtz band structure of di-tetramethyltetraselenafulvalene-X* $[(TMTSF)_2 X]$ *: Role of the basis set*. Zap. Nautn. Sem.Leningrad. Otdel. Mat. Inst. Steklov., **134**(3), 206–210.

[30] Veerman, J. J., et al. (2000, March 14). *On Brillouin zones*. Comm. Math. Phys., **212**(3), 725–744.

[31] Trott, M. (2000). *The Mathematica GuideBook: Graphics in Mathematica*. New York: Springer-Verlag.

[32] Misner, C. W., Thorne, K. S., & Wheeler, J. A. (1973). *Gravitation*. San Francisco: W. H. Freeman.